
Systematic improvement of neural network quantum states using a Lanczos recursion

Hongwei Chen^{1,2} Douglas Hendry¹ Phillip Weinberg¹ Adrian E. Feiguin¹
¹Northeastern University, ² SLAC National Accelerator Laboratory
 {chen.hongw, hendry.d, p.weinberg, a.feiguin}@northeastern.edu

Abstract

The quantum many-body problem lies at the center of the most important open challenges in condensed matter, quantum chemistry, atomic, nuclear, and high-energy physics. While quantum Monte Carlo, when applicable, remains the most powerful numerical technique capable of treating dozens or hundreds of degrees of freedom with high accuracy, it is restricted to models that are not afflicted by the infamous sign problem. A powerful alternative that has emerged in recent years is the use of neural networks as variational estimators for quantum states. In this work, we propose a symmetry-projected variational solution in the form of linear combinations of simple restricted Boltzmann machines. This construction allows one to explore states outside of the original variational manifold and increase the representation power with moderate computational effort. Besides allowing one to restore spatial symmetries, an expansion in terms of Krylov states using a Lanczos recursion offers a solution that can further improve the quantum state accuracy. We illustrate these ideas with an application to the Heisenberg $J_1 - J_2$ model on the square lattice, a paradigmatic problem under debate in condensed matter physics, and achieve start-of-the-art accuracy in the representation of the ground state.

1 Introduction

Understanding correlated quantum systems requires dealing with a large configuration space: datasets are comprised of all possible electronic configurations $\vec{\sigma}$ and cannot be stored in the memory of the largest supercomputer. Hence, the quantum many-body problem can be interpreted as an “extreme data science” problem [13] from an information processing perspective. In a quantum wave function, each electronic or spin configuration has an associated complex amplitude $\psi(\vec{\sigma})$ determined by solving for the eigenvectors of the Hamiltonian operator. In particular, if one is interested in the zero temperature properties of the system, the solution is given by the eigenvector with the smallest eigenvalue. Finding the exact solution of a N quantum bit system with interactions requires solving for the eigenvectors of a $2^N \times 2^N$ matrix. Alternatively, one can formulate the calculation as an optimization problem in which an “energy functional” $E(\psi)$ has to be minimized with respect to all the 2^N complex amplitudes.

Since the number of configurations d grows exponentially with the number of degrees of freedom (electrons, spins), this problem quickly becomes intractable. A solution consists of “compressing” the wave function by proposing a suitable guess for the amplitudes based on some variational parameters $\vec{\alpha} = (\alpha_1, \alpha_2, \dots, \alpha_m)$. Typically, a functional form $\psi(\vec{\sigma}) = f(\vec{\sigma}, \vec{\alpha})$ based on some physical intuition is utilized to represent the amplitude of given configuration/state $\vec{\sigma}$. The optimal parameters α_i are determined by solving the system of equations $\nabla_{\alpha} E = 0$. The objective of this solution is to achieve the lowest possible energy with a number of parameters $m \ll d$.

Some relatively simple wave functions have enjoyed various degrees of success in the past, such as those of the Jastrow type where the amplitudes can be written as pair products $f(\vec{\sigma}, \vec{\alpha}) =$

$\prod_{ij} U(\alpha_{ij} \sigma_i \sigma_j)$. However, in recent years we have witnessed impressive developments based on the use of neural network (NN) wave functions as variational estimators [4], which have jump started of a new vibrant field of research dubbed as “quantum machine learning”. Notice that the optimization of the wave function parameters now translates into the “training” of the NN by minimizing the energy functional that becomes a cost function (we describe the training process below). The power of NN wave functions lies on their complex non-linear structure that provides them with remarkable expressivity to represent arbitrary complex many-body states by, at the same time, being completely agnostic to the physics.

Since restricted Boltzmann machines (RBM) were originally used as a variational ansatz for finding the ground state of the quantum many body systems [4], there has been a growing effort to investigate other forms of neural networks, including convolutional neural networks (CNN) [9], recurrent neural networks (RNN) [19], transformers [23], to mention a few. Thus, neural network quantum states (NNQS) become the most appealing numerical alternative to treat quantum many body systems since they can be systematically improved by adding new layers or hidden variables, for instance. In addition to the ground state search, the application of NNQS ranges from classical simulation of quantum circuits [1, 5, 30], calculation of spectral function [17, 18], thermodynamics simulation [16, 29], and quantum tomography [42].

Contributions In this work, we show how one can use a mathematically simple structure, a restricted Boltzmann machine (RBM), and yet obtain values of the ground state energy that beat all previous estimates by a range of numerical methods, including using convolutional neural networks. As we describe below, instead of increasing the number of layers or hidden variables, the solution lies on considering linear combinations of RBMs. The new wave function allows one to explore a much larger space of solutions. In particular, one can use this construction to restore spatial symmetries [38, 9, 26, 27]. In addition, we propose implementing a projection method based on a Lanczos recursion using a “Krylov basis” of RBMs obtained by sequentially applying powers of the Hamiltonian operator.

The paper is organized as follows: In Sec. 2.1 we describe the quantum many-body problem in the context of the Heisenberg model; in Sec. 2.2 we summarize prior attempts to study this problem using NNQS; in Sec. 3 we review the basic formalism, including the structure of neural network wave functions, how to incorporate the symmetries of the problem into the quantum many-body state, and the numerical training procedure to optimize it. In Sec. 4 we present results of state of the art calculations for the $J_1 - J_2$ Heisenberg model on the square lattice and compare to other numerical techniques. We finally close with a summary and conclusions.

2 The quantum many-body problem

2.1 Model

In the following, we will focus on quantum spin problems where the degrees of freedom σ_i can assume two possible values $\pm 1/2$ (or “up” and “down”). Similarly, one can think of them as generic two-level systems or “qubits”. In particular, we will benchmark our methods in the context of the spin $\frac{1}{2}$ antiferromagnetic Heisenberg model with nearest and next nearest neighbor interactions, the so-called $J_1 - J_2$ model defined by the Hamiltonian:

$$\hat{H} = J_1 \sum_{\langle ij \rangle} \vec{S}_i \cdot \vec{S}_j + J_2 \sum_{\langle\langle ij \rangle\rangle} \vec{S}_i \cdot \vec{S}_j, \quad (1)$$

where $\vec{S} = (\hat{S}^x, \hat{S}^y, \hat{S}^z)$ are spin operators, the first term runs over nearest neighboring sites $\langle ij \rangle$ on a square lattice and the second term runs over next nearest pairs $\langle\langle ij \rangle\rangle$ along the diagonals of the plaquettes. For convenience, in the following we set $J_1 = 1$ as the unit of energy. In this problem, the number of possible configurations grows as $d = 2^N$. However, the ground state wave function lies on the sector with the same number of up and down spins, constraining our search to a smaller subset of states, albeit still exponentially large.

Without the J_2 term, the problem can be numerically solved for hundreds of spins using quantum Monte Carlo (QMC) [36]. However, the method cannot be applied to problems with frustration since it is noticeably affected by the infamous sign problem [22]. In our case, this is due to the presence of

the J_2 term that makes some transition probabilities ill defined (negative). The ground states of this model are well established in two extreme cases: at small J_2/J_1 the system antiferromagnetically orders with wave vector $\mathbf{q} = (\pi, \pi)$; at large J_2/J_1 spins prefer columnar order $\mathbf{q} = (\pi, 0), (0, \pi)$, in which they are aligned antiparallel in one direction, but ferromagnetically in the other. However, in the maximally frustrated regime $J_1 \sim 0.5J_2$, the system does not display any apparent order and the nature of this spin liquid state remains controversial despite significant research effort over the past three decades[3, 6, 11, 10, 33, 37, 39, 32, 35, 24, 20, 15, 21, 43].

Therefore, we choose this Hamiltonian for two reasons: (i) it realizes a quantum spin liquid in a parameter regime near $J_2 \sim 0.5J_1$ and (ii) conventional Monte Carlo methods fail, making the model an ideal testing ground to benchmark new techniques. Variational Monte Carlo (VMC) provides a suitable alternative that can be scaled up to large two-dimensional systems without being affected by the sign problem. The quest for relatively simple but yet powerful variational states has focused on neural network states, which have shown a great deal of promise. The complexity of the problem lies in the fact that many states with similar energy have very different physical properties. Therefore, an accurate representation of the ground state becomes the key to study the nature of the quantum phase.

2.2 Related work

Before the concept of NNQS became a popular new alternative for simulating many-body systems, the most successful numerical techniques to treat the 2D $J_1 - J_2$ model have been the density matrix renormalization group (DMRG)[15], VMC based on a projected fermionic ansatz[20], and tensor product states[43]. Recently, some research has focused on improving the accuracy of NNQS by using deep neural networks such as CNN[9] and group-CNN[34]. The idea of applying quantum number projection to recover the symmetries of the wave function[38, 44] has proven to be effective in improving the performance of NNQS[9, 26, 27, 34]. In addition, other alternatives that enhance the quality of the approximations consist of combining NNQS with Gutzwiller-projected fermionic wave functions[12], or pair-product wave functions[28].

3 Method

3.1 Neural Network Wave Function with symmetry

An RBM wave function takes a spin configuration – a sequence of N values $\pm 1/2$ – and returns a complex coefficient corresponding to the wave function amplitude. In other words, it is a function $\psi : \{-1/2, +1/2\}^N \rightarrow \mathcal{C}$. This function is highly non-linear and is parametrized by biases \vec{a}, \vec{b} and weights W as:

$$\psi(\vec{\sigma}^z, \vec{a}, \vec{b}, W) = e^{\sum_{i=1}^N a_i \sigma_i^z} \prod_{i=1}^M 2 \cosh \left(\sum_{j=1}^N W_{ij} \sigma_j^z + b_i \right). \quad (2)$$

In this expression, the number of “hidden variables” M is a tunable parameter. While RBMs have remained a simple example of a basic neural network for many decades, it was only recently that their potential as variational wave functions was appreciated [4]. In this case, unlike conventional machine learning applications, the biases and weights are complex valued.

It is possible to account for certain symmetries [25] of the problem directly within the internal mathematical structure of the RBM. In particular:

- Spin flip symmetry: If the z -component of the total magnetization is zero ($\sum_i \sigma_i^z = 0$), the global spin flip operation $\sigma_i^z \rightarrow -\sigma_i^z$ preserves this property. Notice that since $\cosh(x)$ is an even function, we can easily restore the global flip symmetry in RBM wave function by removing the “magnetic field” terms associated to biases \vec{a}, \vec{b} in Eq.(2). Thus, the RBM wave function coefficients become:

$$\psi_s(\vec{\sigma}^z, W) = \prod_{i=1}^M 2 \cosh \left(\sum_{j=1}^N W_{ij} \sigma_j^z \right). \quad (3)$$

- Translational symmetry: In translationally invariant systems, the ground state of the Hamiltonian is expected to preserve the translational symmetry of the lattice. By applying the

Table 1: Character table of the C_{4v} point group for square lattice.

| | E | $2C_4$ | C_2 | $2\sigma_v$ | $2\sigma_d$ |
|-------|-----|--------|-------|-------------|-------------|
| A_1 | 1 | 1 | 1 | 1 | 1 |
| A_2 | 1 | 1 | 1 | -1 | -1 |
| B_1 | 1 | -1 | 1 | 1 | -1 |
| B_2 | 1 | -1 | 1 | -1 | 1 |
| E | 2 | 0 | -2 | 0 | 0 |

momentum projection, one can construct a variational wave function that preserved the symmetry with a well defined momentum \mathbf{K} :

$$\psi_{\mathbf{K}} = \sum_{\mathbf{R}} e^{-i\mathbf{K}\cdot\mathbf{R}} \psi_s(T_{\mathbf{R}}\vec{\sigma}^z, W), \quad (4)$$

where the translation operator $T_{\mathbf{R}}$ shift all particles by a distance \mathbf{R} . For the 2D square lattice,

$$\mathbf{R} = m\hat{x} + n\hat{y}. \quad (5)$$

The operator $T_{\mathbf{R}}$ will perform a translation by m steps in the \hat{x} direction, and n steps in the \hat{y} direction. The coefficient $\psi_{\mathbf{K}}$ now satisfies the translational symmetry at the cost of requiring a computation time N time larger.

- Lattice point symmetry: As our target model is on the 2D square lattice, the point group symmetries may also be included:

$$\psi_{\mathbf{K}\mathcal{L}} = \sum_{\mathbf{R}, \mathcal{L}} e^{-i\mathbf{K}\cdot\mathbf{R}} \chi(\mathcal{L}) \psi_s(T_{\mathbf{R}}\mathcal{L}\vec{\sigma}^z, W), \quad (6)$$

where \mathcal{L} is the symmetry operation in the C_{4v} point group, and $\chi(\mathcal{L})$ is the character of the irreducible representation I for the symmetry operation \mathcal{L} . Since there are 8 operations in the C_{4v} point group, as shown in table 1, $\psi_{\mathbf{K}\mathcal{L}}$ is 8 times more expensive to calculate compared to $\psi_{\mathbf{K}}$.

Notice that even though the computational cost of optimizing and evaluating observables with the symmetrized wave function has increased, the resulting state has a much larger expressivity than the original one, translating into a remarkable accuracy as we shall demonstrate. We should highlight here that the new states, by being linear combinations of RBMs, are no longer RBMs, and therefore allow one to explore a much larger space outside the original manifold defined by ψ_s , Eq.(2).

3.2 Wave Function Optimization

The goal of the calculation is to minimize the cost function defined by the expectation value of the energy:

$$E_{var} = \frac{\langle \psi_{\mathbf{K}\mathcal{L}} | H | \psi_{\mathbf{K}\mathcal{L}} \rangle}{\langle \psi_{\mathbf{K}\mathcal{L}} | \psi_{\mathbf{K}\mathcal{L}} \rangle} \quad (7)$$

$$= \sum_{\vec{\sigma}} P_{\vec{\sigma}} E_{loc}(\vec{\sigma}), \quad (8)$$

where the probability distribution is determined by the normalized wave function coefficients

$$P_{\vec{\sigma}} = \frac{|\langle \vec{\sigma} | \psi_{\mathbf{K}\mathcal{L}} \rangle|^2}{\sum_{\vec{\sigma}'} |\langle \vec{\sigma}' | \psi_{\mathbf{K}\mathcal{L}} \rangle|^2} \quad (9)$$

and the local energy is given by

$$E_{loc}(\vec{\sigma}) = \frac{\langle \vec{\sigma} | H | \psi_{\mathbf{K}\mathcal{L}} \rangle}{\langle \vec{\sigma} | \psi_{\mathbf{K}\mathcal{L}} \rangle}. \quad (10)$$

By formulating the problem in probabilistic terms, one can resort to Metropolis-Hastings Markov Chain Monte Carlo to evaluate the averages. The sampling over the spin configurations $\vec{\sigma}$ is carried out by randomly flipping pairs of anti-aligned spins, and using von Neumann rejection according to a transition probability $W = |\langle \vec{\sigma}_{new} | \psi_{\mathbf{K}\mathcal{L}} \rangle|^2 / |\langle \vec{\sigma}_{old} | \psi_{\mathbf{K}\mathcal{L}} \rangle|^2$.

The wave function optimization can be implemented by a variety of methods. Since the energy landscape is extremely complex, simple gradient descent tends to get trapped into metastable solutions. More sophisticated strategies are usually employed, such as natural gradient descent or ‘‘stochastic reconfiguration’’[40]. In contrast to the ‘‘standard’’ natural gradient descent method, the Fubini-study metric[31], which is the complex-valued form of Fisher information, is used to measure the ‘‘distance’’ between wave functions $|\psi\rangle$ and $|\phi\rangle$:

$$\gamma(\psi, \phi) = \arccos \sqrt{\frac{\langle \psi | \phi \rangle \langle \phi | \psi \rangle}{\langle \psi | \psi \rangle \langle \phi | \phi \rangle}}. \quad (11)$$

The procedure to update variational parameters using natural gradient descent is well described in literature[4, 8, 28], and we hereby summarize it. The optimization is done by minimizing the Fubini-study metric between $|e^{-d\tau H} \psi(\theta)\rangle$ and $|\psi(\theta + \delta\theta)\rangle$ where $d\tau$ is a small step in imaginary time and can be viewed as learning rate in the training of neural network. The optimal choice for $\delta\theta$ is given by the solution of a system of equations:

$$\sum_{k'} \left[\langle O_k^\dagger O_{k'} \rangle - \langle O_k^\dagger \rangle \langle O_{k'} \rangle \right] \delta\theta_{k'} = -d\tau \left[\langle O_k^\dagger H \rangle - \langle O_k^\dagger \rangle \langle H \rangle \right], \quad (12)$$

where the log derivative $O_k = \frac{1}{\psi(\theta)} \frac{\partial \psi(\theta)}{\partial \theta}$ and $\langle \dots \rangle$ means an average over samples. We update the parameters by $\theta_k = \theta'_k + \delta\theta_k$ and repeat until convergence is reached.

3.3 Lanczos recursion

Using the symmetrized RBM wave function combined with the stochastic reconfiguration method, a good approximation of the ground state can be achieved after hundreds or thousands iterations. However, due to the limited representation power of neural network wave functions, and the errors stemming from the Monte carlo sampling and the optimization method, the true ground state of the Hamiltonian H can still differ significantly from the variational one. One possible way to increase the expressivity of the wave function is to introduce additional hidden variables or layers. However, an alternative to systematically improve the neural network wave function consists of applying a modified Lanczos recursion [14, 2, 20]. The procedure begins with a (normalized) trial wave function ψ_0 , which in our case is an initial guess for the ground state, $\psi_0 = \psi_{\mathbf{KL}}$. Then, a new state ψ_1 is constructed by applying the Hamiltonian on ψ_0 and subtracting the projection over ψ_0 in order to preserve orthogonality:

$$\psi_1 = \frac{H\psi_0 - \langle H \rangle \psi_0}{(\langle H^2 \rangle - \langle H \rangle^2)^{1/2}} \quad (13)$$

where $\langle H^n \rangle = \langle \psi_0 | H^n | \psi_0 \rangle$. Notice that ψ_1 is orthogonal to ψ_0 and also normalized. In the usual Lanczos method, this recursion can be continued such that a new complete orthogonal basis can be constructed. In this representation, the Hamiltonian will have tri-diagonal form. However, we only use ψ_0 and ψ_1 as our basis, and thus the Hamiltonian will be a 2×2 matrix.

The eigenvector $\tilde{\psi}_0$ that corresponds to the lowest eigenvalue \tilde{E}_0 of this matrix will be a better approximation of the true ground state of Hamiltonian compared to ψ_0 . The lowest eigenvalue and corresponding eigenvector are

$$\tilde{E}_0 = \langle H \rangle + v\alpha \quad (14)$$

$$\tilde{\psi}_0 = \frac{1}{(1 + \alpha^2)^{1/2}} \psi_0 + \frac{\alpha}{(1 + \alpha^2)^{1/2}} \psi_1, \quad (15)$$

where

$$v = (\langle H^2 \rangle - \langle H \rangle^2)^{1/2} \quad (16)$$

$$r = \frac{\langle H^3 \rangle - 3\langle H^2 \rangle \langle H \rangle + 2\langle H \rangle^3}{(\langle H^2 \rangle - \langle H \rangle^2)^{3/2}} \quad (17)$$

$$\alpha = r - (r^2 + 1)^{1/2} \quad (18)$$

The eigenvector $\tilde{\psi}_0$, being a linear combination of ψ_0 and ψ_1 , is the improved neural network wave function, and \tilde{E}_0 is the new improved variational energy. By considering $\tilde{\psi}_0$ as the new trial

Table 2: Ground state energy per site E/N and the spin structure factor $S(\mathbf{q})$ obtained by our RBM wave function, CNN[9], and exact diagonalization[37] for the $J_1 - J_2$ model on 6×6 square lattice. p represents the number of Lanczos steps applied.

| 6×6 | $J_2 = 0.5$ | $J_2 = 0.55$ | $J_2 = 0.6$ |
|-----------------------|-------------|--------------|-------------|
| Energy(Exact) | -0.503810 | -0.495178 | -0.493239 |
| Energy(CNN) | -0.50185(1) | -0.49067(2) | -0.49023(1) |
| Energy(RBM) | -0.50364(2) | -0.49501(1) | -0.49298(5) |
| Energy(RBM) $p = 1$ | -0.50376(3) | -0.49512(4) | -0.49313(5) |
| Energy(RBM) $p = 2$ | -0.50378(4) | -0.49514(4) | -0.49318(5) |
| $S(\pi, \pi)$ (Exact) | 1.16989 | 0.89452 | 0.5545 |
| $S(\pi, \pi)$ (RBM) | 1.177(8) | 0.902(6) | 0.555(4) |
| $S(\pi, 0)$ (Exact) | 0.201907 | 0.2489 | 0.48412 |
| $S(\pi, 0)$ (RBM) | 0.200(2) | 0.246(2) | 0.486(6) |

wave function replacing ψ_0 , this method can be repeated to further improve the neural network wave function. The neural network wave function obtained during the Lanczos recursion can be generalized as

$$|\Psi_p\rangle = (1 + \sum_{i=1}^p \beta_i H^i) |\psi_0\rangle, \quad (19)$$

where p is maximum number of Lanczos steps, and β_i is the wave function coefficient corresponding to $H^i |\psi_0\rangle$. In this form, one can easily identify the wave function as an expansion in a Krylov basis.

In practice, taking into account the fact that the computational complexity increases dramatically with increasing p , only a few steps can be calculated for large quantum many body system. In this study, and for illustration purposes, we shall consider only the $p = 1$ or $p = 2$ cases.

3.4 Implementation details

In this work, we focus on the 2D $J_1 J_2$ Heisenberg model on $L \times L$ square lattices where L is an even number. For the neural network, we use $\psi_{\mathbf{K}\mathcal{L}}$ in all simulations and consider three different values for the number hidden variables M consisting of 2, 2.5 and 3 times of the number of spins $N = L^2$ in the system. The parameters \mathbf{W} in the RBM are initialized to be randomly chosen random numbers with a uniform distribution between $[-0.01, 0.01]$ for both real and imaginary parts. The ground state can belong to the A_1 or B_1 irreducible representations of the C_{4v} point group, depending on the value of J_2/J_1 . In our calculations we consider both cases near the transition between the spin liquid phase and the columnar phase with $\mathbf{K} = (\pi, 0)$, *i. e.* for $J_2/J_1 \geq 0.5$.

Due to the large number of parameters and the numerical noise in sampling, we implement the conjugate gradient method to solve the system of equations, Eq.(12). To stabilize the method, we introduce a ridge parameter $\lambda = 10^{-6}$. For each training step, we collect 10000 samples to evaluate averages as mentioned in Sec. 3.2 including the variational energy and log derivatives. Since the adjacent states in the Markov chain are highly correlated, the number of the skipped states between samples N_{skip} is chosen according to this relation $N_{skip} = 5 \times 1.0/r$, where r is the acceptance rate in the previous training step. The typical value for N_{skip} is from 30 to 100. As for evaluation, we collect 2×10^5 samples to calculate the average and statistical error. The learning rate used in the training ranges from 5×10^{-4} to 3×10^{-2} . Once we observe that variational energy is not decreasing, a smaller learning rate(half of previous one) is used instead. For large L , to save training time, we initialize the parameters \mathbf{W} in $\psi_{\mathbf{K}\mathcal{L}}$ using the parameters trained by means of the cheaper wave function ψ_s . All simulations are performed using Eigen and Intel MKL on Intel E5-2680v4 and AMD Rome 7702 CPU nodes.

4 Results

4.1 Comparison with Exact Diagonalization

We benchmark the accuracy of the neural network wave functions for the ground state mainly on the 6×6 and 10×10 square lattices with periodic boundary conditions. For the 6×6 lattice, the

Table 3: Comparison of the ground state energy per site E/N and the spin structure factor $S(\mathbf{q})$ with QMC[36] results for the 2D Heisenberg model($J_2 = 0$) on 6×6 , 8×8 and 10×10 square lattice.

| System Size | Energy(QMC) | $S(\pi, \pi)$ (QMC) | Energy(RBM) | $S(\pi, \pi)$ (RBM) |
|----------------|--------------|---------------------|--------------|---------------------|
| 6×6 | -0.678873(4) | 2.51799(6) | -0.678868(2) | 2.51(2) |
| 8×8 | -0.673487(4) | 3.7939(2) | -0.673482(3) | 3.79(4) |
| 10×10 | 0.671549(4) | 5.3124(3) | -0.671519(4) | 5.38(6) |

Table 4: Ground state energy per site E/N and the spin structure factor $S(\mathbf{q})$ obtained by our RBM wave function, CNN[9], VMC[20], and DMRG[15] for the $J_1 - J_2$ model on 10×10 square lattice. p represents the number of Lanczos steps applied.

| 10×10 | $J_2 = 0.45$ | $J_2 = 0.5$ | $J_2 = 0.55$ |
|---------------------|--------------|-------------|--------------|
| Energy(VMC) | -0.50811(1) | -0.49521(1) | -0.48335(1) |
| Energy(DMRG) | -0.507976 | -0.495530 | -0.485434 |
| Energy(CNN) | -0.50905(1) | -0.49516(1) | -0.48277(1) |
| Energy(RBM) | -0.50916(2) | -0.49580(2) | -0.48410(3) |
| Energy(RBM) $p = 1$ | -0.5099(5) | -0.4968(4) | -0.4859(5) |
| $S(\pi, \pi)$ (RBM) | 2.06(3) | 1.56(2) | 1.18(2) |
| $S(\pi, 0)$ (RBM) | 0.186(1) | 0.191(2) | 0.200(2) |

$J_1 - J_2$ is numerically soluble by enumerating the possible spin configurations, constructing the Hamiltonian matrix, and explicitly solving the eigenvalue problem [37]. Once the ground state (or its variational approximation) is obtained, the wave function can be used to calculate other physical quantities besides the energy. Here, for illustration, we compute the spin structure factor, that defines the sublattice magnetization squared for a finite system

$$S(\mathbf{q}) = \frac{1}{N^2} \sum_{i,j} \langle \sigma_i^z \sigma_j^z \rangle e^{i\mathbf{q} \cdot (\mathbf{r}_i - \mathbf{r}_j)}, \quad (20)$$

where the wave vector \mathbf{q} determines spatial structure of the magnetic order. Notice that in all the tables shown here, we display the results times a factor N for readability.

We first focus on the symmetrized RBM wave function without the Lanczos optimization, and we start by comparing the ground state energy for a 6×6 lattice as a function of J_2/J_1 , as shown in Fig. 1. In this figure we calculate the relative error as $|E_{nn} - E_{exact}|/|E_{exact}|$ using the exact ground state energy from Ref. [37]. We also include the relative error of the ground state energy obtained using a convolutional neural network wave function from Ref.[9]. While the relative error of the CNNs are in order of 10^{-3} , our RBM wave function achieves an accuracy of 10^{-4} in the frustrated regime.

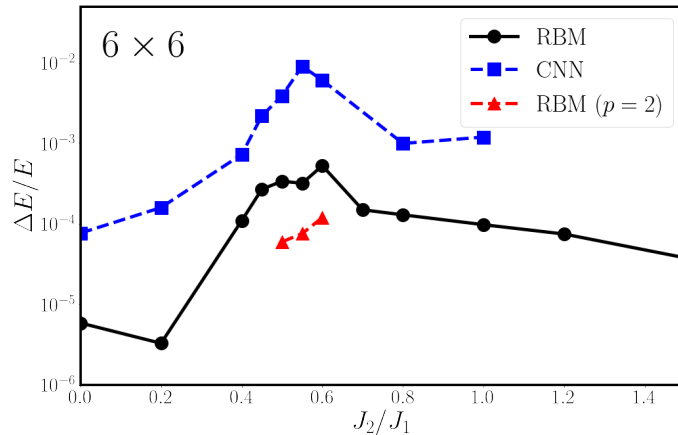


Figure 1: Relative error in the ground state energy obtained with variational Monte Carlo using symmetrized RBM wave functions (this work) and convolutional neural network (CNN) wave functions, from Ref. [9].

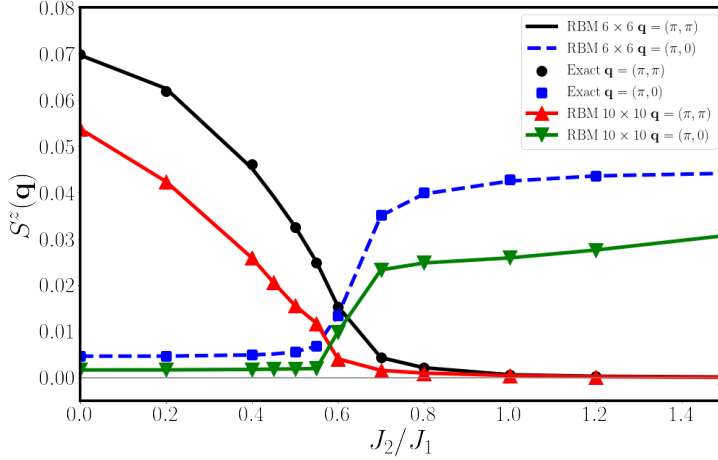


Figure 2: Static spin structure factor for ordering wave vectors $\mathbf{q} = (\pi, \pi)$ and $(\pi, 0)$ obtained with VMC using symmetrized RBM wave functions, compared to numerically exact results on a 6×6 lattice as a function of J_2/J_1 . We also include VMC results for 10×10 . Monte Carlo sampling errors are smaller than the symbol size.

Even comparing other recent works using CNNs[41, 34, 7], our RBM wave function still outperforms the CNN wave function. Besides the ground state energy, the spin structure factor computed from optimized wave functions agree very well with the exact solution as shown in Fig. 2, where the differences are smaller than the symbol size, and in data table 2.

4.2 Comparison with state-of-the-art quantum Monte Carlo

For larger lattices, the problem is numerically intractable. However, as mentioned before, it can be solved using QMC[36] for $J_2 = 0$. Thus, for the case without frustration we can compare with QMC results for several different lattice sizes. From table 3, we can see that even on the 10×10 lattice the energy difference is about 3×10^{-5} , showing the extraordinary accuracy of our RBM wave function.

For the frustrated case, $J_2 \neq 0$, we compare to other methods, such as those obtained with CNN wave functions as well as results using the density matrix renormalization group(DMRG) method with $SU(2)$ symmetry from Ref. [15] and VMC using an Abrikosov-fermion mean field with a Z_2 gauge structure from Ref. [20]. From the data tables 4 and 5, we observe that our RBM wave function outperform the CNN wave function again in the entire range of J_2/J_1 . In the frustrated regime, comparisons with VMC and DMRG using all the data available in literature demonstrate that the RBM wave functions still yield competitive ground state energies except at $J_2/J_1 = 0.55$ where DMRG yields a lower value.

4.3 Lanczos optimization

Since the most interesting regime lies around the maximally frustrated point $J_2 \sim 0.5J_1$, we choose 3 different values of J_2/J_1 using 6×6 and 10×10 lattices and perform a few Lanczos steps to further improve the ground state energy. From data table 2 and 4, we see that the Lanczos steps are very effective regardless of the system size. Remarkably, by performing $p = 1$ Lanczos steps, we obtain better energy at $J_2/J_1 = 0.55$ for the 10×10 lattice that improves significantly the best available data using state of the art DMRG, as shown in data table 4. Moreover, on the 6×6 lattice at $J_2/J_1 = 0.55$, we obtain a variational energy of -0.49514(4), to be compared to the ‘‘RBM+PP’’ calculation from Ref.[28], -0.495075(1) where a combination of neural network and projected entangled pair states are used as variational ansatz. Additionally, with the help of the Lanczos recursion, a better estimate of the energy can be obtained by carrying out a variance extrapolation as illustrated in Ref. [2, 20]. We also try to improve the estimation of spin structure factor using Lanczos, but the Monte Carlo sampling error makes the improvement not obvious.

Table 5: Ground state energy per site E/N and the spin structure factor $S(\mathbf{q})$ obtained by our RBM wave function, exact diagonalization[37], and CNN[9] for the $J_1 - J_2$ model on 6×6 and 10×10 square lattice.

| 6×6 | $J_2 = 0.0$ | $J_2 = 0.2$ | $J_2 = 0.4$ | $J_2 = 0.45$ | $J_2 = 0.7$ |
|-----------------------|--------------|--------------|--------------|--------------|--------------|
| Energy(Exact) | -0.678872 | -0.599046 | -0.529745 | -0.51565739 | -0.530001 |
| Energy(CNN) | -0.67882(1) | -0.59895(1) | -0.52936(1) | -0.51452(1) | - |
| Energy(RBM) | -0.678868(2) | -0.599044(3) | -0.529687(7) | -0.51552(1) | -0.529921(8) |
| $S(\pi, \pi)$ (Exact) | 2.5180 | 2.22946 | 1.6604 | - | 0.15605 |
| $S(\pi, \pi)$ (RBM) | 2.51(2) | 2.25(2) | 1.63(2) | 1.412(8) | 0.1567(7) |
| $S(\pi, 0)$ (Exact) | 0.167453 | 0.1691 | 0.17784 | - | 1.26743 |
| $S(\pi, 0)$ (RBM) | 0.1678(7) | 0.1681(7) | 0.1774(8) | 0.1845(8) | 1.26(2) |
| 6×6 | $J_2 = 0.8$ | $J_2 = 1.0$ | $J_2 = 1.2$ | $J_2 = 1.5$ | |
| Energy(Exact) | -0.586487 | -0.714360 | -0.848364 | -1.05268 | |
| Energy(CNN) | -0.58590(1) | -0.71351(1) | - | - | |
| Energy(RBM) | -0.586411(9) | -0.71429(1) | -0.84830(1) | -1.052640(9) | |
| $S(\pi, \pi)$ (Exact) | 0.07726 | 0.02318 | 0.01115 | 0.00557 | |
| $S(\pi, \pi)$ (RBM) | 0.0779(4) | 0.0233(2) | 0.0110(1) | 0.00556(5) | |
| $S(\pi, 0)$ (Exact) | 1.4402 | 1.54318 | 1.5729 | 1.59 | |
| $S(\pi, 0)$ (RBM) | 1.43(2) | 1.53(2) | 1.57(2) | 1.59(2) | |
| 10×10 | $J_2 = 0.0$ | $J_2 = 0.2$ | $J_2 = 0.4$ | $J_2 = 0.6$ | $J_2 = 0.7$ |
| Energy(CNN) | -0.67135(1) | -0.59275(1) | -0.52371(1) | -0.47604(1) | - |
| Energy(RBM) | -0.671519(4) | -0.592847(9) | -0.52388(2) | -0.47662(3) | -0.51889(2) |
| $S(\pi, \pi)$ (RBM) | 5.38(6) | 4.24(5) | 2.59(4) | 0.408(3) | 0.1594(9) |
| $S(\pi, 0)$ (RBM) | 0.1684(9) | 0.1702(8) | 0.180(2) | 0.99(2) | 2.33(7) |
| 10×10 | $J_2 = 0.8$ | $J_2 = 1.0$ | $J_2 = 1.2$ | $J_2 = 1.5$ | |
| Energy(CNN) | -0.57383(1) | -0.69636(1) | - | - | |
| Energy(RBM) | -0.57404(2) | -0.69670(2) | -0.82565(3) | -1.02371(3) | |
| $S(\pi, \pi)$ (RBM) | 0.1004(5) | 0.0480(2) | 0.0212(2) | 0.00760(6) | |
| $S(\pi, 0)$ (RBM) | 2.48(7) | 2.59(5) | 2.76(5) | 3.07(5) | |

5 Conclusion

Neural network wave functions hold a great deal of promise due to their ability to compress complex quantum many body states within a relatively simple mathematical structure that, owed to its non-linearity, can encode an exponentially large amount of information with polynomial resources. In particular, RBM wave functions, initially deemed too simple, can be used as building blocks for systematically improved wave functions. These improved states obey the internal symmetries of the model and the point group symmetries of the lattice. In addition, they may contain contributions from states living in a ‘‘tangent space’’ to the original RBM manifold. These tangent vectors are spanned in terms of powers of the Hamiltonian and form a Krylov basis.

We have demonstrated that we can achieve state of the art accuracy that improves previous results using convolutional neural networks with a minimal amount of extra computational cost compared to simple RBMs. The combination of Lanczos and symmetrization offer a relatively cheap and effective solution to problems previously beyond reach of the most powerful numerical techniques and provide the means to bypass the sign problem. These ideas can seamlessly translate to other areas of research ranging from materials science to quantum chemistry. Besides, our variational solution can be adopted to calculate the excitation spectrum of a quantum many-body system[17, 18], providing valuable information that can be directly compared to experiments.

Limitations The computational cost of a single training step scales as $\mathcal{O}(N_{sample} \times MN^2)$, where the number of hidden variables M is usually proportional to the system size N . Thus, the computation time of the calculation may be a bottleneck for its application on larger lattices.

Negative Societal Impact Our work presents the theoretical simulation of the quantum many-body problems without any foreseeable negative societal impacts.

Acknowledgments and Disclosure of Funding

AEF and HC acknowledge the National Science Foundation for support under grant No. DMR-1807814. DH is partially supported by a Northeastern Tier 1 grant.

References

- [1] Johannes Bausch. Recurrent quantum neural networks. *Advances in neural information processing systems*, 33:1368–1379, 2020.
- [2] Federico Becca, Wen-Jun Hu, Yasir Iqbal, Alberto Parola, Didier Poilblanc, and Sandro Sorella. Lanczos steps to improve variational wave functions. *Journal of Physics: Conference Series*, 640:012039, sep 2015.
- [3] Luca Capriotti and Sandro Sorella. Spontaneous plaquette dimerization in the j_1 - j_2 heisenberg model. *Physical Review Letters*, 84(14):3173, 2000.
- [4] Giuseppe Carleo and Matthias Troyer. Solving the quantum many-body problem with artificial neural networks. *Science*, 355(6325):602–606, 2017.
- [5] Juan Carrasquilla, Di Luo, Felipe Pérez, Ashley Milsted, Bryan K Clark, Maksims Volkovs, and Leandro Aolita. Probabilistic simulation of quantum circuits using a deep-learning architecture. *Physical Review A*, 104(3):032610, 2021.
- [6] P Chandra and B Doucot. Possible spin-liquid state at large s for the frustrated square heisenberg lattice. *Physical Review B*, 38(13):9335, 1988.
- [7] Ao Chen, Kenny Choo, Nikita Astrakhantsev, and Titus Neupert. Neural network evolution strategy for solving quantum sign structures. *Physical Review Research*, 4(2):L022026, 2022.
- [8] Kenny Choo, Giuseppe Carleo, Nicolas Regnault, and Titus Neupert. Symmetries and many-body excitations with neural-network quantum states. *Phys. Rev. Lett.*, 121:167204, Oct 2018.
- [9] Kenny Choo, Titus Neupert, and Giuseppe Carleo. Two-dimensional frustrated J_1 - J_2 model studied with neural network quantum states. *Phys. Rev. B*, 100:125124, Sep 2019.
- [10] Elbio Dagotto and Adriana Moreo. Phase diagram of the frustrated spin-1/2 heisenberg antiferromagnet in 2 dimensions. *Phys. Rev. Lett.*, 63:2148–2151, Nov 1989.
- [11] R Darradi, O Derzhko, R Zinke, J Schulenburg, SE Krüger, and J Richter. Ground state phases of the spin-1/2 j_1 - j_2 heisenberg antiferromagnet on the square lattice: A high-order coupled cluster treatment. *Physical Review B*, 78(21):214415, 2008.
- [12] Francesco Ferrari, Federico Becca, and Juan Carrasquilla. Neural gutzwiller-projected variational wave functions. *Phys. Rev. B*, 100:125131, Sep 2019.
- [13] J. K. Freericks, B. K. Nikolić, and O. Frieder. The nonequilibrium quantum many-body problem as a paradigm for extreme data science. *International Journal of Modern Physics B*, 28(31):1430021, 2014.
- [14] Eduardo R. Gagliano, Elbio Dagotto, Adriana Moreo, and Francisco C. Alcaraz. Correlation functions of the antiferromagnetic heisenberg model using a modified lanczos method. *Phys. Rev. B*, 34:1677–1682, Aug 1986.
- [15] Shou-Shu Gong, Wei Zhu, D. N. Sheng, Olexei I. Motrunich, and Matthew P. A. Fisher. Plaquette ordered phase and quantum phase diagram in the spin- $\frac{1}{2}$ J_1 - J_2 square heisenberg model. *Phys. Rev. Lett.*, 113:027201, Jul 2014.
- [16] Douglas Hendry, Hongwei Chen, and Adrian Feiguin. Neural network representation for minimally entangled typical thermal states. *arXiv preprint arXiv:2204.11904*, 2022.
- [17] Douglas Hendry, Hongwei Chen, Phillip Weinberg, and Adrian E. Feiguin. Chebyshev expansion of spectral functions using restricted boltzmann machines. *Phys. Rev. B*, 104:205130, Nov 2021.
- [18] Douglas Hendry and Adrian E. Feiguin. Machine learning approach to dynamical properties of quantum many-body systems. *Phys. Rev. B*, 100:245123, Dec 2019.
- [19] Mohamed Hibat-Allah, Martin Ganahl, Lauren E. Hayward, Roger G. Melko, and Juan Carrasquilla. Recurrent neural network wave functions. *Phys. Rev. Research*, 2:023358, Jun 2020.

- [20] Wen-Jun Hu, Federico Becca, Alberto Parola, and Sandro Sorella. Direct evidence for a gapless Z_2 spin liquid by frustrating néel antiferromagnetism. *Phys. Rev. B*, 88:060402, Aug 2013.
- [21] Hong-Chen Jiang, Hong Yao, and Leon Balents. Spin liquid ground state of the spin-1 2 square j 1-j 2 heisenberg model. *Physical Review B*, 86(2):024424, 2012.
- [22] EY Loh Jr, JE Gubernatis, RT Scalettar, SR White, DJ Scalapino, and RL Sugar. Sign problem in the numerical simulation of many-electron systems. *Physical Review B*, 41(13):9301, 1990.
- [23] Di Luo, Zhuo Chen, Kaiwen Hu, Zhizhen Zhao, Vera Mikyoung Hur, and Bryan K Clark. Gauge invariant autoregressive neural networks for quantum lattice models. *arXiv preprint arXiv:2101.07243*, 2021.
- [24] Matthieu Mambrini, Andreas Läuchli, Didier Poilblanc, and Frédéric Mila. Plaquette valence-bond crystal in the frustrated heisenberg quantum antiferromagnet on the square lattice. *Physical Review B*, 74(14):144422, 2006.
- [25] Takahiro Mizusaki and Masatoshi Imada. Quantum-number projection in the path-integral renormalization group method. *Physical Review B*, 69(12):125110, 2004.
- [26] Yusuke Nomura. Machine learning quantum states — extensions to fermion–boson coupled systems and excited-state calculations. *Journal of the Physical Society of Japan*, 89(5):054706, 2020.
- [27] Yusuke Nomura. Helping restricted boltzmann machines with quantum-state representation by restoring symmetry. *Journal of Physics: Condensed Matter*, 33(17):174003, apr 2021.
- [28] Yusuke Nomura and Masatoshi Imada. Dirac-type nodal spin liquid revealed by refined quantum many-body solver using neural-network wave function, correlation ratio, and level spectroscopy. *Physical Review X*, 11(3):031034, 2021.
- [29] Yusuke Nomura, Nobuyuki Yoshioka, and Franco Nori. Purifying deep boltzmann machines for thermal quantum states. *Physical Review Letters*, 127(6):060601, 2021.
- [30] Mateusz Ostaszewski, Lea M Trenkwalder, Wojciech Masarczyk, Eleanor Scerri, and Vedran Dunjko. Reinforcement learning for optimization of variational quantum circuit architectures. *Advances in Neural Information Processing Systems*, 34:18182–18194, 2021.
- [31] JP Provost and G Vallee. Riemannian structure on manifolds of quantum states. *Communications in Mathematical Physics*, 76(3):289–301, 1980.
- [32] N Read and Subir Sachdev. Large-n expansion for frustrated quantum antiferromagnets. *Physical review letters*, 66(13):1773, 1991.
- [33] J Richter and J Schulenburg. The spin-1/2 j1–j2 heisenberg antiferromagnet on the square lattice: Exact diagonalization for n= 40 spins. *The European Physical Journal B*, 73(1):117–124, 2010.
- [34] Christopher Roth and Allan H MacDonald. Group convolutional neural networks improve quantum state accuracy. *arXiv preprint arXiv:2104.05085*, 2021.
- [35] Subir Sachdev and RN Bhatt. Bond-operator representation of quantum spins: Mean-field theory of frustrated quantum heisenberg antiferromagnets. *Physical Review B*, 41(13):9323, 1990.
- [36] Anders W. Sandvik. Finite-size scaling of the ground-state parameters of the two-dimensional heisenberg model. *Phys. Rev. B*, 56:11678–11690, Nov 1997.
- [37] HJ Schulz, TAL Ziman, and Didier Poilblanc. Magnetic order and disorder in the frustrated quantum heisenberg antiferromagnet in two dimensions. *Journal de Physique I*, 6(5):675–703, 1996.
- [38] Hao Shi, Carlos A Jiménez-Hoyos, R Rodríguez-Guzmán, Gustavo E Scuseria, and Shiwei Zhang. Symmetry-projected wave functions in quantum monte carlo calculations. *Physical Review B*, 89(12):125129, 2014.
- [39] J Sirker, Zheng Weihong, OP Sushkov, and J Oitmaa. J 1- j 2 model: First-order phase transition versus deconfinement of spinons. *Physical Review B*, 73(18):184420, 2006.
- [40] Sandro Sorella and Luca Capriotti. Green function monte carlo with stochastic reconfiguration: An effective remedy for the sign problem. *Physical Review B*, 61(4):2599, 2000.
- [41] Attila Szabó and Claudio Castellano. Neural network wave functions and the sign problem. *Phys. Rev. Research*, 2:033075, Jul 2020.

- [42] Giacomo Torlai, Guglielmo Mazzola, Juan Carrasquilla, Matthias Troyer, Roger Melko, and Giuseppe Carleo. Neural-network quantum state tomography. *Nature Physics*, 14(5):447–450, 2018.
- [43] Ling Wang, Zheng-Cheng Gu, Frank Verstraete, and Xiao-Gang Wen. Tensor-product state approach to spin- $\frac{1}{2}$ square J_1-J_2 antiferromagnetic heisenberg model: Evidence for deconfined quantum criticality. *Phys. Rev. B*, 94:075143, Aug 2016.
- [44] Hui-Hai Zhao, Kota Ido, Satoshi Morita, and Masatoshi Imada. Variational monte carlo method for fermionic models combined with tensor networks and applications to the hole-doped two-dimensional hubbard model. *Physical Review B*, 96(8):085103, 2017.